SMALL-SCALE SOLAR MAGNETIC FIELDS

J. O. STENFLO
Lund Observatory, Lund, Sweden

Abstract. The observed properties of small-scale solar magnetic fields are reviewed. Most of the magnetic flux in the photosphere is in the form of strong fields of about 100–200 mT (1–2 kG), which have remarkably similar properties regardless of whether they occur in active or quiet regions. These fields are associated with strong atmospheric heating. Flux concentrations decay at a rate of about 10^7 Wb s^{-1}, independent of the amount of flux in the decaying structure. The decay occurs by smaller flux fragments breaking loose from the larger ones, i.e. a transfer of magnetic flux from smaller to larger Fourier wave numbers, into the wave-number regime where ohmic diffusion becomes significant. This takes place in a time-scale much shorter than the length of the solar cycle.

The field amplification occurs mainly below the solar surface, since very little magnetic flux appears in diffuse form in the photosphere, and the life-time of the smallest flux elements is very short. The observations further suggest that most of the magnetic flux in quiet regions is supplied directly from below the solar surface rather than being the result of turbulent diffusion of active-region magnetic fields.

1. Introduction

Solar magnetic fields are of fundamental importance for most solar phenomena. The solar cycle itself is a manifestation of the interaction between solar rotation, convection, and magnetic fields. It is thus not surprising that most review papers in solar physics contain discussions of magnetic fields, including their small-scale properties. Recent reviews with fairly extensive discussion of small-scale fields have been given by Harvey (1971, 1974), Stenflo (1971), Severny (1972), Mullan (1974), and Deubner (1975). The emphasis in many of these papers has however been on observed structures substantially larger than one arcsec, whereas the true sizes of the basic magnetic elements in the network and plages appear to be considerably smaller. Most values of the field strengths that have been quoted have been of limited value since the relation between the observed and true field strengths has not been clear.

During the past few years a new picture of solar magnetic fields has gradually emerged due to advances in observational techniques and in the theoretical understanding of the Zeeman effect in the solar atmosphere. According to this picture, there are hardly any weak magnetic fields in the photosphere (where the magnetic field is measured). Most of the net magnetic flux is carried by fields of 100–200 mT (1–2 kG), even when the average field strength is much less than 1 mT (10 G). The corresponding magnetic elements occupy only a tiny fraction of the solar surface and have sizes in quiet regions generally less than 200 km. Much of the discussion in the present review will be focused on the properties of the basic subarcsec magnetic elements, i.e. on scales comparable to the size of Bohemia or less. A spatial resolution of 100 km is considered to be exceedingly poor and completely inadequate in Earth studies, while such a resolution has never been achieved for the Sun. The best spatial resolution in direct magnetograph observations has been about 1000 km so far.

Bumba and Kleczek (eds.), Basic Mechanisms of Solar Activity, 69–99.

The unresolved fine structure in the magnetic field has introduced errors in determinations of the average field strengths from magnetograph observations. This error has earlier often been considered to be a nuisance and an obstacle that should be removed to allow the magnetic-field structure to be determined more accurately. We now realize, however, that the error in itself is a powerful diagnostic tool and even seems to contain more information about the true structure of the magnetic field than the direct observations.

The deduced magnetic pressure in the magnetic elements apparently exceeds the ambient gas pressure in the photosphere and the dynamic pressure due to motions of the solar plasma. The generation of such an extreme fine structure poses a fundamental plasma physics problem. Further, as we shall see, the small-scale nature of solar magnetic fields affects our views on the dynamics and energy balance of the solar atmosphere, as well as our understanding of differential rotation and the solar cycle.

2. Observed Properties of Small-Scale Solar Magnetic Fields

2.1. True field strengths

The signal from a solar magnetograph recording the circular polarization in a line wing is a measure of the magnetic flux, *not* of the field strength. The apparent flux values need to be corrected to represent the true net flux through the scanning aperture of a magnetograph, but this correction is generally less than a factor of two (Howard and Stenflo, 1972). By dividing the net flux through the aperture by the aperture area, we arrive at an *apparent* field strength, B_{obs}. As most of the magnetic flux through the solar surface appears to be channelled through subarcsec elements (see Section 2.3), which have never been spatially resolved by any magnetograph, the directly recorded field strengths B_{obs} alone do not provide much information on the true field strengths except that they may indicate some lower limits. In this sense the 'direct' methods of mapping solar magnetic fields do not represent the most direct ways of determining the field strengths. For this purpose the 'line-ratio' method is more adequate (see Section 2.1.2). Both methods will be reviewed in the following sections.

A typical example of the best spatial resolution presently achieved in magnetograph observations is given in Figure 1, due to Vrabec (1974).

2.1.1. *Direct Observations*

Various approaches to determine the true magnetic field strengths directly have been tried. Stenflo (1966, 1968a) and Severny (1967) made repeated scans of the same regions with different sizes of the scanning aperture. The results showed that the apparent field strengths increased rapidly with decreasing aperture size down to the smallest apertures that could be used then, 7 $(\text{arcsec})^2$. It was however not clear how far this increase would continue if one could go down to infinitely small aperture sizes.

Many authors have tried to measure the apparent field strengths with the highest spatial resolution available at the best seeing conditions. Sheeley (1966, 1967) found field strengths in the quiet region network in excess of 30 mT (300 G). The diameters

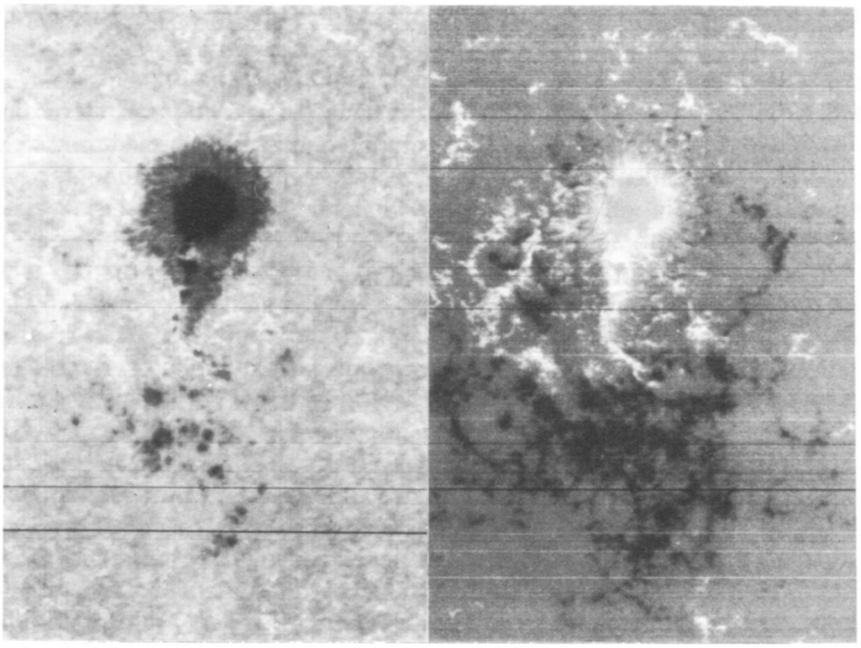

Fig. 1. Magnetogram (right) of the active region shown to the left, obtained on January 9, 1971 at the Aerospace San Fernando Solar Observatory by D. Vrabec and T. Janssens (Vrabec, 1974). This magnetogram gives an impression of the highest spatial resolution that can be achieved in present magnetograph observations. It shows a complex pattern of flux elements imbedded in a virtually field-free photosphere.

of the flux concentrations were often less than one arcsec. In active regions Beckers and Schröter (1968a) found numerous flux concentrations with typical diameters of 1000 km and observed field strengths in the range 60–140 *mT*. These strong-field regions appeared to carry most of the magnetic flux occurring outside the sunspots. Similar results, including the evolution and dynamics of the flux concentrations, have been presented by Vrabec (1971, 1974), who finds that the small flux elements are imbedded in a virtually field-free photosphere.

Filtergram observations generally allow a higher spatial resolution than magnetograph observations due to the shorter integration times (which reduces the seeing effects). As there is a one-to-one correspondence between brightness enhancements and concentrations of magnetic flux (see Section 2.8), one can measure the sizes of the bright points and compare with magnetic flux recordings, to get an estimate of the field strengths. This requires however that one can resolve the individual bright points and assume that the brightness structures and magnetic elements are of the same size, which is far from obvious. Simon and Zirker (1974) tried to measure the sizes of the magnetic structures observed in high-resolution spectrograms and found typical apparent dimensions of 1–2″. As this is much larger than the sizes of the 'filigree' structures earlier recorded in $H\alpha$ filtergrams by Dunn and Zirker (1973), Simon and Zirker (1974) concluded that the magnetic elements are generally larger than the brightness elements. Model calculations of Stenflo

https://doi.org/10.1017/S0074180900008081 Published online by Cambridge University Press

(1974b, 1975) indicate on the other hand that the brightness enhancements are spread out over a somewhat larger area than the associated magnetic flux (see Section 2.8).

Mehltretter (1974) counted the number of resolved bright points in filtergrams and compared with the observed magnetic flux in the region. This procedure gave a flux of 4×10^9 Wb per element. As the typical size of a bright point was about the same as or less than the resolution of the telescope (Sacramento Peak Observatory vacuum tower) and microphotometer, i.e. 140 km, Mehltretter estimated the typical field strength of a bright point to be 200–250 mT (2–2.5 kG).

As the Zeeman splitting is proportional to the square of the wavelength, it is advantageous to use infrared lines, which may be completely split in the flux elements, while spectral lines in the visible are only partially split (overlapping sigma components). By using the line Fe I λ 1.5648 μm, Harvey and Hall (1975) obtained evidence that the flux elements have field strengths of typically 150–200 mT (1.5–2 kG) inside as well as outside active regions.

A further indication that the true field strengths are quite high is obtained from observations of pores and the umbrae of small sunspots. Steshenko (1967) found $B_{\text{obs}} \approx 140\ mT$ (1.4 kG) for the smallest pores he could observe (1.5–2″). This seemed to be a lower limit for the field strength in sunspots. Bumba (1967) found $B_{\text{obs}} \approx 160$–$210\ mT$ in pores and spots of diameter 1000–3000 km. Both Steshenko and Bumba noted that the observed field strength increases only slowly with increasing sunspot area.

2.1.2. *The Line-Ratio Method*

Calibrating a solar magnetograph means to find the relation between the circular polarization recorded at a fixed position in the line wing and the magnetic flux through the scanning aperture. This relation (the calibration curve) is a linear one for small field strengths, but deviates strongly from linearity (Zeeman saturation) when the Zeeman splitting becomes comparable to the line width. Even in the case of weak fields, the magnetograph signal is sensitive to the shape of the line profile. When a magnetograph is calibrated directly, the observed *average* line profile is used. Due to the pronounced concentration of magnetic flux to small regions, the average profiles are typical for the non-magnetic regions. We know that there are indeed large changes in the line profiles in magnetic regions, visible as line 'gaps' (Sheeley, 1967) in spectrograms (see Section 2.8).

Straightforward interpretations of magnetograms using calibration curves based on average line profiles are generally in error due to the combined effects of Zeeman saturation, line weakenings in magnetic regions, and uncompensated Doppler shifts (occurring on a scale smaller than the spatial resolution). Unfortunately it has not been possible to calibrate magnetographs using the line profiles in magnetic regions, since the magnetic elements are far too small to be resolved by magnetographs or in spectrograms. Many people have considered this as a serious principle limitation of magnetograph observations. Instead it turns out that the 'error' in the flux determination contains information about the unresolved small-scale magnetic structures. This source of information can be tapped using the line-ratio method without the

need for achieving extremely high spatial resolution or working at excellent seeing conditions.

The line-ratio method uses simultaneous magnetograph recordings in two or more properly selected spectral lines. Since the scanning aperture, telescope and spectrograph are the same for the different lines, and the observations are made simultaneously, smearing effects due to seeing and instrument resolution will be the same for the pair of lines chosen. The apparent field strengths recorded in the two lines will be different due to difference in Zeeman saturation, line weakenings, uncompensated Doppler shifts, and height of line formation. A comparison between apparent field strengths in two spectral lines can thus give information on these parameters. By a careful choice of pairs of spectral lines, the various effects mentioned can be untangled.

The methods of extracting information from the magnetograph 'calibration error' were developed by Stenflo (1968b) and have since been improved when applied to various sets of data (Harvey and Livingston, 1969; Howard and Stenflo, 1972; Frazier and Stenflo, 1972; Gopasyuk *et al.*, 1973; Caccin *et al.*, 1974; Frazier, 1974; Stenflo, 1971, 1973, 1974b, 1975).

Before the nature of the magnetic fine structure was known, it was natural to assume that there should be all kinds of magnetic elements in the photosphere, of all sizes and field strengths from zero to several hundred *mT*. Similarly a continuous distribution of temperature enhancements and Doppler shifts in the magnetic elements would be expected. As a general approach to such an inhomogeneous atmosphere, Stenflo (1968b) introduced a 'multi-component' model, each component occupying a certain fraction of the scanning aperture and having a given field strength distribution (Zeeman saturation), temperature enhancement (line weakening), and velocity (uncompensated Doppler shift). Following suggestions by Alfvén (1967), a filamentary model was considered as a special case of this general approach. We will presently consider such a 'two-component' model in some detail, since it has proven to represent the situation in the photosphere remarkably well and will be repeatedly referred to in our discussions of observational data.

Accordingly, we assume that there are two types of regions on the Sun: strong and weak-field regions. If Φ is the net longitudinal magnetic flux through the scanning aperture, we can write

$$\Phi = \Phi_s + \Phi_w, \tag{1}$$

Φ_s being the flux in strong-field form, and Φ_w the corresponding weak-field flux. The magnetograph calibration is correct for the weak-field flux, since the calibration refers to average line profiles, and the weak fields occupy the major fraction of the solar surface. For the strong-field regions, the magnetograph calibration is in error by a factor δ, determined by Zeeman saturation, line weakenings, and uncompensated Doppler shifts.

The observed line-of-sight magnetic field is thus

$$B_{obs} = (\delta \Phi_s + \Phi_w)/A, \tag{2}$$

A being the aperture area, while the true average field is

$$\bar{B} = \Phi/A. \tag{3}$$

https://doi.org/10.1017/S0074180900008081 Published online by Cambridge University Press

If we define the average strength $\bar{B}_w$ of the weak-field component

$$\bar{B}_w = \Phi_w / A, \tag{4}$$

we find, using (1)–(4),

$$B_{obs} = \delta \bar{B} + (1-\delta)\bar{B}_w. \tag{5}$$

The commonly used line for magnetograph observations, Fe I λ 525.02 nm, is quite susceptible to Zeeman saturation, temperature enhancements, and Doppler shifts, causing δ to be considerably smaller than unity. The Fe I λ 523.3 nm line is on the other hand insensitive to these effects (except in the line core), being much broader and having considerably smaller Landé factor than the 525.0 nm line. As δ for the 523.3 nm line is thus approximately unity, which has been verified by more detailed model calculations (Stenflo, 1975), $B_{523.3}$ represents a good approximation for the average field $\bar{B}$, and (5) can be written

$$B_{525.0} = \delta_{525.0} B_{523.3} + (1-\delta_{525.0})\bar{B}_w. \tag{6}$$

An example of a scatter-plot diagram of $B_{525.0}$ vs. $B_{523.3}$ is shown in Figure 2, taken from Frazier and Stenflo (1972). The difference in intercepts of the lines fitted to the positive and negative points provides information on $\bar{B}_w$ (see Section 2.3).

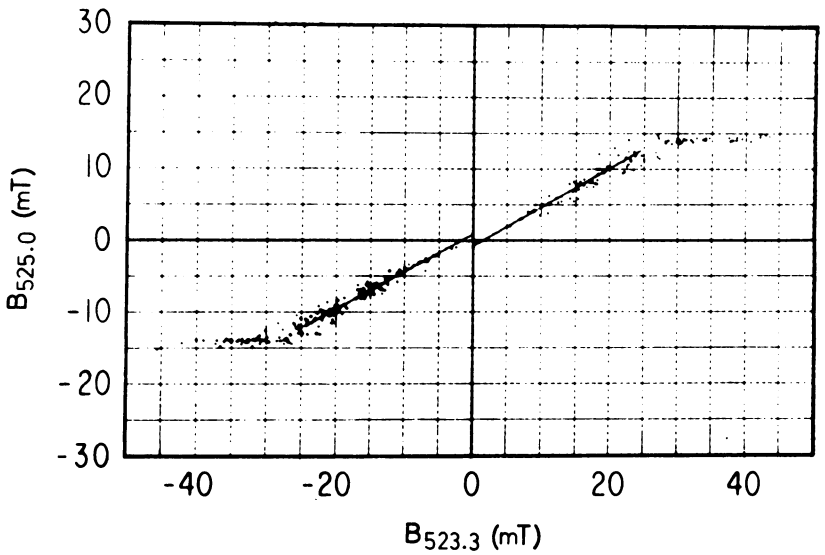

Fig. 2. Scatter-plot diagram of $B_{525.0}$ vs. $B_{523.3}$ for the brighter plage structures in an active region. Two straight lines have been fitted to the positive and negative points. Points with $|B_{523.3}| > 25\ mT$ contain an instrumental saturation in the $B_{525.0}$ channel and have not been used when fitting the straight lines. From Frazier and Stenflo (1972).

If the two-component model were too idealized, the real Sun containing a large range of various types of magnetic elements, we would have a broad distribution of values of δ. The points in a diagram giving $B_{525.0}$ vs. $B_{523.3}$ would then not fall along a straight line representing a single δ value, but there would be a large scatter in the

https://doi.org/10.1017/S0074180900008081 Published online by Cambridge University Press

diagram. The absence of such a scatter in excess of the instrumental noise provides empirical justification for the simple two-component model (see Section 2.2).

The effect of Zeeman saturation on the value of δ contains the information on the true field strengths in the flux concentrations. To extract this information we must find a method to separate out Zeeman saturation from the other factors affecting the slope in the scatter-plot diagrams. This is done by choosing a pair of lines which should behave identically in all respects except for the sensitivity to Zeeman saturation. Two such lines are Fe I λ 525.02 nm and Fe I λ 524.71 nm. Both belong to the same multiplet, have practically the same excitation potential of the lower level, the same oscillator strength and equivalent width. The only essential difference between the lines is their effective Landé factors, 3.0 for the 525.0 nm line, and 2.0 for the 524.7 nm line. Simultaneous recordings in these two lines have been made by Stenflo (1973) for a quiet region at disk center. If $\bar{B}_w$ in (5) is small compared with B_{obs}, it may be neglected when determining the slope k in the $B_{525.0}-B_{524.7}$ scatter-plot diagram. In this case

$$k \approx \delta_{525.0}/\delta_{524.7}. \tag{7}$$

k can differ from unity only if there are strong, unresolved magnetic fields inside the scanning aperture. As the 525.0 nm line is more sensitive to Zeeman saturation, we expect that k should be less than unity and be smallest when the magnetograph exit slits are closest to the line core, increasing towards unity when the exit slits are moved further out in the wings. This effect is observed, supporting the validity of the interpretation.

The longitudinal magnetic field in a flux element can be described by giving the peak value of the field strength at the center of the element and the shape of the magnetic cross-section. The relation between the slope k and the peak field strength is sensitive to the assumed shape of the cross-section. Assuming a cylindrically-symmetric magnetic element, four different magnetic profiles have been considered:

(1) Gaussian cross-section

$$B = B_0\, e^{-(r/r_0)^2}. \tag{8}$$

(2) The profile

$$B = B_0[1-(r/r_0)^2]^2. \tag{9}$$

(3) The profile

$$B = B_0[1-(r/r_0)^2]. \tag{10}$$

(4) Single-valued field $B = B_0$ throughout the element.

The values of B_0 derived from the observed slope k were 230, 186, 167, and 110 mT, respectively, for the four types of magnetic cross-sections mentioned above (Stenflo, 1973, 1975). The value 110 mT represents a definite lower limit. This result should be contrasted with the fact that most of the field strengths $B_{525.0}$ observed with the $2.4 \times 2.4''$ scanning aperture were considerably smaller than 1 mT, not a single of the 1943 points in the raster having an apparent field in excess of 5 mT (Stenflo, 1973). This apparent contradiction is understood only if the sizes of the magnetic elements are very small compared with the size of the scanning aperture (see Section 2.5).

https://doi.org/10.1017/S0074180900008081 Published online by Cambridge University Press

The derivation of B_0 from k is not model dependent except for the assumed magnetic cross-section. Various atmosphere models (Milne-Eddington, HSRA, etc.) give practically identical results (Stenflo, 1975), because the Zeeman saturation is a simple manifestation of the fact that the separation between the σ components becomes comparable to the line width. The total half-width of the lines we consider is about 10 *pm* (100 mÅ), and does not vary greatly with atmospheric model. The relation between Zeeman splitting and field strength depends in a well-known way on atomic parameters.

Harvey *et al.* (1972) made recordings of the complete line profiles of the Stokes I and V parameters for the 525.0 nm line and used these observations to derive average field strengths of 50 mT (500 G) in the unresolved magnetic elements, but needed to introduce a dispersion in the field strengths of about 100 mT. If magnetic profiles like (8)–(10) are used instead of characterizing the magnetic elements by an average field strength plus a dispersion, practically the same field strengths as those derived from the slope in the 525.0–524.7 scatter-plot diagram are obtained (Stenflo, 1973).

Wiehr and Wittmann (1975) have recently used a pair of spectral lines belonging to a different multiplet to isolate the effect of Zeeman saturation, and have found approximately the same high values of the field strengths in the magnetic elements.

Frazier (1974) combined Stenflo's (1973) observations with velocity data and showed that the maximum field strength B_0 within a flux concentration must be between 130 and 260 mT in order to satisfy both the magnetic and velocity data (see Section 2.7).

2.2. Uniqueness of the field strength distribution

The flux elements appear to have remarkably unique and universal properties. This conclusion is mainly based on the following observations:

(1) The points in the 525.0–523.3 scatter-plot diagram fall along a straight line. No systematic deviation from linearity is observed for $B_{523.3} < 20\ mT$ (Harvey and Livingston, 1969; Frazier and Stenflo, 1972).

(2) The scatter of the points around this straight line does not appreciably exceed the scatter due to random instrumental noise, which was 0.1–0.2 mT for the quiet-region scan analysed (Frazier and Stenflo, 1972).

(3) The straight line has practically the same slope in quiet as in active regions (excluding sunspots) (Frazier and Stenflo, 1972).

Argument (1) shows that $\delta_{525.0}$ is independent of the average field strength in the scanning aperture, at least as long as $B_{523.3} \lesssim 20\ mT$. The amount of Zeeman saturation, line weakenings, and uncompensated Doppler shifts are thus independent of the amount of magnetic flux within the aperture. This indicates that there is no intrinsic change in the physical parameters between different regions when we measure apparently different magnetic fluxes and enhancements in the photospheric brightness. The conclusion that the physical parameters are independent of the amount of magnetic flux is supported by argument (3) above, according to which the Zeeman saturation plus other effects appear to be the same in quiet regions as in active-region plages.

Argument (2) above indicates that the intrinsic scatter of the physical parameters characterizing the magnetic elements must be small compared with the average values ($\Delta B_0/\bar{B}_0 \ll 1$, etc.).

If the temperature enhancement in magnetic regions is independent of the amount of magnetic flux, we should expect a linear relation between apparent brightness enhancement $\Delta I/\bar{I}$ and apparent field strength $B_{523.3}$. The observed relations (Frazier, 1971) are shown in Figure 3 for brightness enhancements in the continuum as well as in the core of Fe I λ 525.0 nm. The scatter of the points is large, particularly for the continuum due to the superposed non-magnetic brightness fluctuations in the granulation, but average curves can be fitted to the good statistical sample of points.

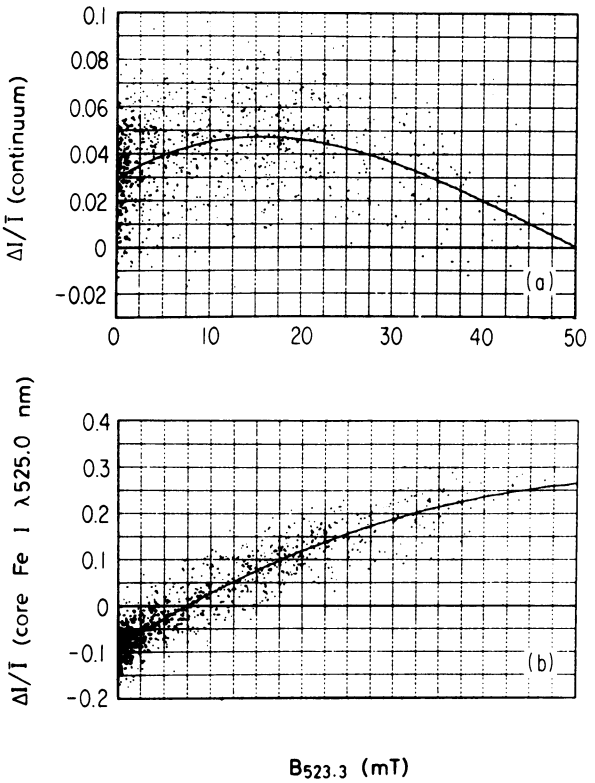

Fig. 3. Relations between observed brightness enhancement $\Delta I/\bar{I}$ and observed magnetic field $B_{523.3}$. (a) Continuum brightness. (b) Core brightness for Fe I λ 525.0 nm. From Frazier (1971).

The relation between observed magnetic field and brightness enhancement in the continuum is linear only up to $B_{523.3} \approx 5\ mT$ (possibly $10\ mT$). The brightness enhancement reaches a maximum around $B_{523.3} \approx 15\ mT$ and then decreases. This decline corresponds to a gradual transition to pores and sunspots as more magnetic flux occurs within the aperture (Frazier, 1971; Stenflo, 1975).

The enhancement in core brightness does not show such a decline for large values of the observed magnetic flux, but only a slight deviation from linearity when the

https://doi.org/10.1017/S0074180900008081 Published online by Cambridge University Press

observed field strength $B_{523.3}$ exceeds 30 mT. This degree of linearity is consistent with the observed linear relation between $B_{525.0}$ and $B_{523.3}$ for $B_{523.3} \lesssim 20$ mT.

The magnetograph signal is fairly insensitive to variations in the continuum brightness, which explains why deviations from linearity in the continuum enhancement are not seen in the $B_{525.0} - B_{523.3}$ scatter-plot diagram. The behaviour of the continuum intensity shows that intrinsic changes in temperature and density in the lower photosphere are not independent of the amount of magnetic flux in a given region. It is remarkable, however, that the magnetic field strengths and line weakenings (temperatures and densities in the *upper* photosphere) appear to remain almost entirely independent of the amount of magnetic flux, at least for $B_{523.3} < 20$ mT.

Chapman (1974) has pointed out another, more qualitative argument in favor of the uniqueness of the field-strength distribution. He observes that there is no consistent difference in appearance of dark $H\alpha$ fibrils lying on or near the magnetic features, although the apparent field strength of the features varies between 1 and 40 mT.

2.3. Proportion of magnetic flux in strong-field form

Howard and Stenflo (1972) and Frazier and Stenflo (1972) concluded from an analysis of simultaneous magnetograph recordings in the two lines Fe I λλ 525.0 and 523.3 nm that more than 90% of the total magnetic flux through the solar surface recorded by the magnetographs is chanelled through the strong-field regions. As this conclusion has quite far-reaching theoretical implications, we will explain the arguments behind it in some detail.

The aperture sizes used in the two investigations were $17 \times 17''$ and $2.4 \times 2.4''$, respectively, so it is not excluded that a considerable amount of flux is carried by some kind of 'turbulent' magnetic field, which is so tangled that opposite-polarity fluxes almost average out over an area of $2.4 \times 2.4''$. The magnetograph will hardly detect this type of flux unless the resolution is considerably improved (see Section 2.10).

To better understand the nature of the fluxes involved, it is useful to distinguish between two types of weak fields:

(1) Part of the weak-field flux is statistically unrelated to the strong fields.

(2) The remaining part of the weak-field flux is closely correlated with the strong fields, with a polarity either the same or opposite to that of the adjacent strong fields.

In the first case the weak fields will contribute to the scatter around the straight lines in the $B_{525.0} - B_{523.3}$ scatter-plot diagram. If there are no strong-field regions within the scanning aperture, the weak-field points will fall along a straight line with a slope of unity, and will be concentrated near the origin in the diagram. If there are strong fields inside the aperture, the weak-field flux will shift the points from the line of slope $\delta_{525.0}$ towards a line of slope unity, thus contributing to the scatter. In the case of the quiet-region scan of Frazier and Stenflo (1972), for which the highest magnetograph sensitivity was used, the scatter around the straight line of slope $\delta_{525.0}$ did not exceed the instrumental scatter. As the rms instrumental noise was 0.1–0.2 mT, the rms of the random component of $\bar{B}_w$ in (6) should be less than about

https://doi.org/10.1017/S0074180900008081 Published online by Cambridge University Press

0.1 mT. This limit is less stringent for the active-region scans, for which the rms instrumental noise was about 0.8 mT.

The second kind of weak-field flux which is systematically related to the strong fields, is revealed as it causes a systematic displacement of the straight line. Since the sign of $\vec{B}_w$ depends on the sign of the strong fields, the second term in (6) determining the intercept of the straight line should change sign when going from the positive to the negative side of the scatter-plot diagram. If we fit two separate straight lines to the positive and negative points as in Figure 2 and determine the two intercepts l_+ and l_-, we can use (6) to obtain an estimate of the average value of $\vec{B}_w$:

$$\langle \vec{B}_w \rangle = \frac{l_+ - l_-}{2(1-\delta_{525.0})}. \tag{11}$$

A positive value means that $\vec{B}_w$ is systematically of the same sign as the neighbouring strong fields.

$\langle \vec{B}_w \rangle$ has been found to be $\approx -0.08 \pm 0.04$ mT for the quiet-region scan and fluctuates between -0.2 and -0.5 mT for the active-region scans (Frazier and Stenflo, 1972).

As the straight lines fitted to the points in the scatter-plot diagram are mainly determined by points with $|B_{523.3}| \gg |\vec{B}_w|$, the weak fields we are talking about are located immediately adjacent to the strong fields, within the same aperture area. With no strong fields inside the aperture, the points would fall close to the origin in the scatter-plot diagram (or along a line of slope unity, which is not observed), where they do not contribute significantly to the measured value of $\langle \vec{B}_w \rangle$.

The negative values of $\langle \vec{B}_w \rangle$ indicate that the strong fields are immediately surrounded by weak fields of *opposite* polarity. Frazier and Stenflo (1972) interpreted this result in terms of a model of a strong-field region with diverging, 'mushroom'-shaped field lines, part of the magnetic flux returning back to the adjacent photosphere within a distance of a few arcsec.

To estimate the fraction of magnetic flux in strong-field form, the absolute values of the fluxes measured at each of the N aperture positions in a raster are summed up. The ratio ρ between the total fluxes measured in the 525.0 and 523.3 nm lines is

$$\rho = \sum_{i=1}^{N} |\Phi_{525.0}| \Big/ \sum_{i=1}^{N} |\Phi_{523.3}|. \tag{12}$$

As we can assume that the true flux is measured in the 523.3 nm line (cf. the derivation of (6) in Section 2.1.2),

$$\rho = \sum_{i=1}^{N} |\delta\Phi_{s_i} + \Phi_{w_i}| \Big/ \sum_{i=1}^{N} |\Phi_i|, \tag{13}$$

where the notations in (1) have been used.

Let us denote the fraction of the flux in strong-field form by R_s, i.e.

$$R_s = \sum_{i=1}^{N} |\Phi_{s_i}| \Big/ \sum_{i=1}^{N} |\Phi_i|. \tag{14}$$

https://doi.org/10.1017/S0074180900008081 Published online by Cambridge University Press

When strong-field elements are inside the scanning aperture, we can assume that $|\Phi_w| < \delta|\Phi_s|$, so that

$$|\delta\Phi_s + \Phi_w| = \delta|\Phi_s| + \varepsilon|\Phi_w|, \tag{15}$$

where $\varepsilon = +1$ or -1 depending on whether Φ_s and Φ_w are of equal or opposite signs. Away from strong-field elements $\Phi_s = 0$, and (15) is valid with $\varepsilon = 1$. Accordingly

$$\rho = \left(\delta \sum_{i=1}^{N} |\Phi_{s_i}| + \sum_{i=1}^{N} \varepsilon_i |\Phi_{w_i}|\right) \Big/ \sum_{i=1}^{N} |\Phi_i|. \tag{16}$$

Using (14), we have

$$\rho = \delta R_s + \sum_{i=1}^{N} \varepsilon_i |\Phi_{w_i}| \Big/ \sum_{i=1}^{N} |\Phi_i|. \tag{17}$$

Similarly, as $\delta = 1$ implies $\rho = 1$ according to (13) and (1),

$$1 = R_s + \sum_{i=1}^{N} \varepsilon_i |\Phi_{w_i}| \Big/ \sum_{i=1}^{N} |\Phi_i|. \tag{18}$$

Subtraction of (17) and (18) gives

$$R_s = \frac{1-\rho}{1-\delta}. \tag{19}$$

Observations (Frazier and Stenflo, 1972) give for a quiet region at disk center $\rho \approx 0.43$ and $\delta \approx 0.45$, resulting in $R_s \approx 104\%$. The explanation why R_s exceeds 100% is that Φ_s is not a directly observed quantity; for every aperture position weak-field fluxes Φ_w of *opposite* polarity always occur, cancelling out a small fraction of Φ_s. In the definition of R_s in (14), we have used the *observed* total flux $\sum|\Phi|$ in the denominator, which includes the flux cancelling effect inside an aperture area.

It thus appears that the magnetic flux through the solar photosphere in strong-field form is even *larger* than the total flux seen by a magnetograph with a scanning aperture of $2.4 \times 2.4''$ or larger. Part (at least 4%) of the flux seems to return to the solar surface within a distance of $2.4''$ from the strong-field regions. If the magnetograph resolution were infinitely high, the cancelling effect within the aperture would vanish, and R_s should be $\leq 100\%$. Similar results were obtained for the magnetic fields in active regions (Frazier and Stenflo, 1972).

2.4. Question of flux quantization

As there is strong evidence for a unique field-strength distribution characterizing all magnetic elements in the quiet-region network as well as in active-region plages (see Section 2.2), the question naturally arises if there is also a unique amount of magnetic flux assigned to each of the smallest flux elements, in other words if there is flux quantization. Livingston and Harvey (1969) tried to determine the existence of such a flux quantum using a technique similar to the Millikan oil drop method for determining the charge of the electron. They reported some evidence for such a quantization, giving the value 2.8×10^{10} Wb for the flux quantum. This very difficult measurement was based on rather poor statistics, and later work has shown that the flux quantum Φ_0, if it exists at all, must be much smaller.

https://doi.org/10.1017/S0074180900008081 Published online by Cambridge University Press

From an analysis of Stokesmeter data, Harvey *et al.* (1972) tried to derive sizes and field strengths of unresolved magnetic elements. According to their results, the average flux of an element was about 7×10^9 Wb, but both smaller and larger fluxes were found. Although this value is 4 times less than that found by Livingston and Harvey (1969), it should be regarded as an upper limit, since it is not known to what extent the flux concentrations studied represent aggregates of smaller flux elements.

Stenflo (1973) used a different approach to estimate an upper limit for Φ_0 from his $B_{525.0}$–$B_{524.7}$ data. The total observed magnetic flux divided by the area of the scanned quiet region corresponded to a field strength of 0.4 mT. Multiplying by the area of a supergranular cell, the average flux per cell is approximately 3×10^{11} Wb. If the average number of separate flux elements per supergranular cell is n, $\Phi_0 = 3\times10^{11}/n$ Wb. If we can set a lower limit for n, we obtain an upper limit for Φ_0.

As there is a one-to-one correspondence between flux concentrations and bright network points (see Section 2.8), we expect that n should equal the number of bright points making up the intricate filigree pattern of the network around one supergranular cell, as it would appear if seen with infinitely high spatial resolution. To judge from high resolution filtergrams, this number should be of the order of 100, maybe more, which also agrees with estimates of the number of spicules per supergranulation cell (Beckers, 1972; Lynch *et al.*, 1973). If the value of Φ_0 by Livingston and Harvey (1969) were correct, n would only be 10, which is clearly much too small. We estimate that $n \gtrsim 100$ and accordingly $\Phi_0 \lesssim 3\times10^9$ Wb.

Mehltretter (1974) compared the number density of bright facular points in a high-resolution filtergram with the magnetic flux in the same region recorded almost simultaneously at Kitt Peak with a $2.4\times2.4''$ aperture. He estimated the magnetic flux associated with a single facular point to be 4.4×10^9 Wb. This should probably be regarded as an upper limit, since clumps of bright points may not have been resolved, leading to an underestimate of the number density of bright points.

A further estimate, which is much less precise but leads to consistent results, is obtained by comparing large-scale flux measurements with counts of spicules or dark fine mottles, assuming that each such feature is associated with a flux element. The total magnetic flux through the Sun was typically 10^{15} Wb during the period 1967–1973 (Howard, 1974). The total number of dark fine mottles on the Sun is estimated to be about 300 000 (Michard, 1974). All dark fine mottles are likely to be associated with flux elements. The reverse may not be true; there need not be a mottle at every flux element. The total flux divided by the number of dark fine mottles should then be an upper limit for Φ_0, the flux per magnetic element. Accordingly, $\Phi_0 \lesssim 3\times10^9$ Wb.

Considering all these arguments together, we conclude that $\Phi_0 \lesssim 5\times10^9$ Wb, which is a rather conservative estimate of the upper limit. As we will see below (e.g. Section 2.6), it is highly doubtful that the concept of flux quantization is at all physically meaningful, and it should better be abandoned.

2.5. True sizes of magnetic elements

Let us define the size d of a magnetic element by the equation

$$\Phi = B_0 d^2, \tag{20}$$

https://doi.org/10.1017/S0074180900008081 Published online by Cambridge University Press

Φ being the magnetic flux and B_0 the maximum field strength within an element. As B_0 must be in the interval 130 to 260 mT according to Section 2.1.2, and individual flux elements in the network should typically have $\Phi \leq 5 \times 10^9$ Wb according to Section 2.4, we obtain a corresponding upper limit for d by using $B_0 = 130$ mT and $\Phi = 5 \times 10^9$ Wb in (20). The result is

$$d \leq 200 \text{ km}, \tag{21}$$

or $d \leq 0.3''$.

It is not quite clear whether the associated brightness structures are of the same size as the magnetic elements, although more detailed data analysis (Stenflo, 1975) indicates that the brightness structures are slightly larger (see Section 2.8). Dunn and Zirker (1973) recorded at excellent seeing conditions an intricate small-scale brightness pattern in the far wings of Hα, which they called 'solar filigree'. Typical sizes of elements in the filigree pattern were 200 km. As this was about the same as their instrumental resolution, true sizes could not be derived.

Mehltretter (1974), using broad and narrow-band filters in the near UV, recorded photospheric faculae at the center of the solar disk with high spatial resolution. His results suggest that 'solar filigree' are identical with faculae and represent concentrations of magnetic flux. The full half-width of telescope + microphotometer was 140 km. Mehltretter (1974) found that the true half-width of the facular points, after correction for smearing, was about the same as or smaller than the instrumental half-width of 140 km. This result is consistent with our upper limit for d, the size of the magnetic elements. We recall that our estimate of d did not depend on observations with high spatial resolution but was mainly based on field strengths derived using the line-ratio method.

Let us stress that we have been discussing only the smallest flux elements in this section. Larger flux aggregates with correspondingly larger sizes often cannot be regarded as the mere sum of smaller flux fragments but may act cohesively as one single unit. This will be clarified more in the next section.

2.6. Life-times

The life-times of flux concentrations and bright points depend on the size of the feature studied, which explains why various authors have reported highly different results. Mehltretter (1974) finds that his bright facular points with diameters of about 150 km live for 5–15 min. Associations of bright points and 'micropores' have life-times of 10–30 min (Mehltretter, 1974), which agrees with results of Bray and Loughhead (1961), Beckers and Schröter (1968a), and Sheeley (1969). Using the line-ratio method, Howard and Stenflo (1972) found evidence that the life-time of the basic magnetic elements is less than two hours, without being able to set any lower limit.

Assuming that the life-time of the bright elements also represents the life-time of the associated magnetic structures, a decay rate

$$\mathrm{d}\Phi/\mathrm{d}t \approx -10^7 \text{ Wb s}^{-1} \tag{22}$$

appears to account for most of the observational results remarkably well. An element

with $\Phi = 4 \times 10^9$ Wb, typical for the facular points observed by Mehltretter (1974), would decay in a time of about 7 min according to (22), in agreement with Mehltretter's (1974) estimate of 5–15 min. Moving magnetic features (MMF) around sunspots have typical fluxes of 10^{11} Wb each, and seem to endure for hours (Harvey and Harvey, 1973; Vrabec, 1974). According to (22), an element with $\Phi = 10^{11}$ Wb will live for 2–3 h, consistent with the above results. Harvey and Harvey (1973) estimate that the net flux loss from a sunspot through MMFs is $d\Phi/dt \approx -10^{11}$ Wb h^{-1}, i.e. -3×10^7 Wb s^{-1}, which is slightly larger than (22) but of the same order of magnitude. Bumba (1963) and Gokhale and Zwaan (1972) observe that the slowest flux loss from a sunspot, during its most stable phase of decay, is $-(1.2\text{–}1.8) \times 10^7$ Wb s^{-1} independent of the sunspot area, in excellent agreement with (22).

The remarkably universal applicability of the decay rate expressed by the empirical law (22) indicates that sunspots, pores, 'magnetic knots', MMFs, and bright points are not merely to be regarded as an association of individual flux quanta, since the life-time of the aggregate would in that case be about the same as the life-time of its individual elements. Instead the flux aggregate should have some cohesiveness and act as a single physical unit, similar to the flux ropes described by Piddington (1975a, c).

The diffusion time τ_d for an element of size d is

$$\tau_d = \mu_0 \sigma d^2, \tag{23}$$

σ being the electrical conductivity. As the flux Φ is $B_0 d^2$, B_0 being the maximum field strength (cf. (20)), dispersion of the field lines occurs at a characteristic rate of

$$\Phi/\tau_d = B_0/(\mu_0 \sigma). \tag{24}$$

Using the photospheric values of $B_0 = 0.2$ T (see Section 2.1.2) and $\sigma = 10$ mho m^{-1} (Kopecký, 1971), we obtain $\Phi/\tau_d \approx 1.6 \times 10^4$ Wb s^{-1}, which is about three orders of magnitude slower than the decay rate given by our empirical law (22).

It thus appears necessary to invoke some kind of plasma instability occurring on a small scale, to explain the observed fast decay rate of solar magnetic fields. Larger flux concentrations must break up into smaller flux elements, which retain the strong values of the field strength. Otherwise a considerable fraction of the flux would appear in diluted, weak-field form, which is not observed (see Section 2.3). In the Fourier domain the flux moves from small to large wave numbers, where rapid decay may occur. This picture supports the recent suggestion by Piddington (1975a, c) that flux ropes may decay by untwisting and subsequent 'fraying' or separation of flux fibres by the flute instability.

Implications of the decay rate for theories of the solar cycle and for heating of the solar atmosphere will be discussed in Section 3.

2.7 Relation to velocity fields

Flux concentrations always appear to be correlated with downflow of matter, regardless of whether they occur in the quiet-region network (Simon and Leighton, 1964; Tannenbaum *et al.*, 1969; Frazier, 1970) or in active-region plages (Servajean,

1961; Beckers and Schröter, 1968a; Giovanelli and Ramsay, 1971; Sheeley, 1971; Howard, 1971, 1972).The magnitude of these downdrafts is of the order of 0.5 km s^{-1} as observed with a spatial resolution of a few arcsec.

The next question that arises is whether the velocity field has as pronounced a fine structure as the magnetic field. Skumanich *et al.* (1975) found a proportionality between the apparent velocity and the apparent magnetic field: $v_{obs}/B_{obs} \approx 16\ m\ s^{-1}\ mT^{-1}$. If the true maximum field strength in the magnetic elements is $B_0 = 200\ mT$, the peak velocity would be $v_0 = 3.2$ km s^{-1} if the velocity is strictly proportional to the magnetic field at the smallest scale. Such a high value of v_0 seems to be ruled out by stokesmeter observations of Harvey *et al.* (1972) and line-ratio data by Stenflo (1973), indicating that the average downdraft velocity in the magnetic elements is less than 1 km s^{-1}. This apparent contradiction would be resolved if the velocity profile is broader than the corresponding magnetic profile, with a substantial fraction of the downward mass flux occurring immediately outside the magnetic structures. A similar conclusion was reached by Dravins (1974) from a comparison of the visibility of the bright network in the blue and red wings of Hα. Howard (1972) noted a slight tendency for the downward motions to be concentrated over the parts of the flux regions with high gradient of the apparent magnetic field, which is consistent with the above interpretation.

Frazier (1974) employed the line-ratio method to derive information on the velocity profile of the magnetic elements. The apparent downdraft velocities recorded simultaneously in the two lines Fe I $\lambda\lambda$ 525.0 and 523.3 nm are systematically different from each other. Frazier (1974) combined his velocity data with the $B_{525.0}$–$B_{524.7}$ results of Stenflo (1973), and assumed that the profiles of the true line-of-sight velocities $v(r)$ and magnetic fields $B(r)$ are related by

$$v(r) = \alpha B(r)^{\beta} \tag{26}$$

in the case of a cylindrically-symmetric element. r is the distance from the axis of the element. The constant α is fixed by the requirement that the true average downdraft velocity should be 0.5 km s^{-1}, as suggested by Harvey *et al.* (1972) and Stenflo (1973). β is the remaining free parameter to be determined. If β is less than unity, the velocity structures are coarser than the magnetic-field structures.

The value of β was found to be sensitive to the *shape* of the magnetic-field profile, which was not known. The observational data could however only be satisfied for profiles with the peak field strength B_0 in the interval 130 to 260 mT. The value of β decreased with increasing B_0 and was found to be smaller than unity for $B_0 \gtrsim 170\ mT$. For the Gaussian magnetic-field profile ($B_0 = 230\ mT$), $\beta \approx 0.25$. As indirect evidence supports the view that the velocity structures are more extended than the associated magnetic-field structures, i.e. $\beta < 1$, we might tentatively narrow down the allowed interval for B_0 to be between 170 and 260 mT. Let us however add a word of caution: The different levels of height of formation of the 525.0 and 523.3 nm lines were not taken into account by Frazier but may affect the results.

Finally it should be mentioned that the bright network or facular points show transverse motions, as if being shuffled around by the solar granulation over distances of the order of 1000 km (Sheeley, 1969, 1971; Dravins, 1974; Mehltretter, 1974).

2.8. Relation to Temperature and Density Variations

The flux concentrations are always accompanied by line weakenings, both in the quiet-region network (Sheeley, 1967; Chapman and Sheeley, 1968; Harvey and Livingston, 1969; Frazier, 1970; Harvey *et al.*, 1972; Stenflo, 1973, 1974b, 1975) and in active-region plages (Schmahl, 1967; Stellmacher and Wiehr, 1971, 1973; Stenflo, 1974b, 1975). Due to the unique and universal properties of the magnetic elements (see Section 2.2), their temperature and density structure should be essentially the same in quiet as in active regions (if the average observed field strength $B_{523.3} \lesssim 10\ mT$). A facular model should thus be identical with a model of a magnetic element or a model of the quiet-region network. A number of facular models have been constructed in the past, based on continuum and line-profile data (Kuz'minykh, 1964; Schmahl, 1967; Chapman, 1970; Wilson, 1971; Stellmacher and Wiehr, 1971, 1973; Shine and Linsky, 1974). All of these models have however been hampered by the finite spatial resolution of the observations, which have only been able to indicate lower limits to the true brightness enhancements. This serious limitation was avoided by Stenflo (1974b, 1975), by combining continuum and line profile data with magnetograph observations using the line-ratio method. The zero point of the geometrical height scale, which could not be obtained from the observational data available, was chosen by Stenflo (1974b, 1975) in such a way that the temperature difference between the inside and outside of the flux tube is zero at large depths (more precisely at $\tau_0 = 25$, τ_0 being the continuum optical depth at 500 nm). The justification for this is that the narrow flux tube is almost optically thin making it difficult to maintain large temperature differences in the lower layers, where the radiative relaxation time is short (cf. the discussion in Section 3.1).

The resulting model, which satisfies the observational data including the magnetograph observations, shows no temperature deficit in the lower layers. The temperature excess starts at a height of about 180 km above the level where $\tau_0 = 1$ in the Harvard-Smithsonian Reference Atmosphere (HSRA), and increases rapidly with height. It gives line weakenings concentrated to the line core (Stellmacher and Wiehr, 1971, 1973), the neutral lines being considerably more weakened than the ionized lines, as observed by Chapman and Sheeley (1968). It further gives a positive continuum contrast at disk center, in agreement with observations of Schmahl (1967), Frazier (1971), Dunn and Zirker (1973), and Mehltretter (1974). The higher layers appear to be efficiently heated in the flux elements, presumably by MHD waves. This heating may be of fundamental importance for the whole energy-balance of the solar atmosphere (see Section 3.2).

Let us now face the interesting question whether the brightness structures seen in the continuum are coarser than the magnetic-field structures or not. Analogously to the case of magnetic fields and velocities (see Section 2.7), Skumanich *et al.* (1975) found a proportionality between the apparent continuum brightness enhancement at disk center and the apparent magnetic field $B_{\rm obs}$ for $B_{\rm obs} < 12\ mT$: $(\Delta I_c/\bar{I}_c)_{\rm obs}/B_{\rm obs} \approx 9.3 \times 10^{-4}\ mT^{-1}$. If there were strict proportionality between the true brightness enhancement and the true magnetic field at the smallest scale, a peak magnetic field B_0 of 200 mT would correspond to a peak brightness contrast at disk center $\Delta I_c/\bar{I}_c$ of as much as 19%. According to the model calculations of Stenflo (1974b, 1975), the

https://doi.org/10.1017/S0074180900008081 Published online by Cambridge University Press

observational data could not be satisfied if the true average continuum contrast across a magnetic element exceeds 8%. The most probable model had an average contrast of about 6%. This indicates that the diameter of the brightness elements slightly exceeds that of the magnetic elements. Applying the line-ratio method on combined brightness, velocity, and magnetic-field data, a future determination of the shapes of the magnetic, brightness, and velocity profiles should be possible, as indicated in Section 2.7 when discussing the velocity profiles.

Dunn and Zirker (1973) and Mehltretter (1974) found that the bright network and facular points are preferentially located in the intergranular lanes and are associated with abnormal granulation. As the facular material fills the darker intergranular lanes with emission, the contrast in the granulation is washed out. The presence of facular emission at disk center in the continuum can only be discerned in photographs with spatial resolution better than 0.5″ or by sensitive photoelectric recordings, revealing average enhancements in the continuum signal of the order of one percent.

As described in Section 2.2 and by Figure 3, the increase of the continuum brightness turns into a decrease and darkening as larger and larger flux concentrations are considered. This shows again that a large flux concentration is physically different from the sum of a number of smaller flux elements with the same total flux, a conclusion reached in Section 2.6 when studying the life-times of flux aggregates with different amounts of flux. Active cooling seems to be able to reduce the temperatures in the lower layers only when the flux concentration is sufficiently large and optically thick, so that radiative relaxation is slow enough, and the large flux may effectively interact with convection (Stenflo, 1975). According to Figure 3, deviations from a linear relation between continuum brightness flux and magnetic flux start to become significant for $B_{523.3} \gtrsim 10\ mT$, i.e. when more than about 10% of the $2.4 \times 2.4''$ aperture area is occupied by strong-field magnetic flux. Only when more than 30% of the aperture area is covered by the strong fields, the region is darker in the continuum.

Finally we note the close relation between bright network points and spicules. Spicule counts (Beckers, 1972; Lynch *et al.*, 1973) indicate satisfactory agreement with estimates of the number of flux elements, as was noted in Section 2.4. The spicule life-time of 5–15 min (Beckers, 1972) is about the same as the life-time of bright points (see Section 2.6). Each bright point cannot give rise to more than *one* spicule, since it has disappeared before a new spicule can occur. Successive spicules that appear to be ejected from one and the same bright area thus represent an apparent effect caused by the limited spatial resolution.

2.9. Height variation of the magnetic field

Very little is known about the height variation of the field. Straightforward comparison between magnetograph recordings made in lines formed at different heights is not possible, because the generally dominating effects of Zeeman saturation, line weakenings, etc., affect various lines differently. Further, the magnetograph signal is mainly proportional to the flux, not the field strength. Averaged over an area of a few arcsec, the flux from a 0.2″ magnetic element may be the same at different heights,

although the field lines are diverging and the field strength decreases with height.

The most direct way to measure the height variation therefore seems to be to use the line-ratio method. The field strengths derived by Stenflo (1973) from his $B_{525.0} - B_{524.7}$ observations refer to a height of approximately +100 km relative to the height where $\tau_0 = 1$ in HSRA (Stenflo, 1975). By using other pairs of lines formed at different heights, the true height variation may be found. Another way is to study the center-to-limb variation of the $B_{525.0} - B_{524.7}$ and $B_{525.0} - B_{523.3}$ scatter-plot diagrams. The center-to-limb variation of the ratio $B_{525.0}/B_{523.3}$ indicates that the field lines diverge rapidly with height (Howard and Stenflo, 1972). The conclusion that part of the strong-field flux returns in the form of weak-field opposite-polarity flux adjacent to the magnetic elements (Frazier and Stenflo, 1972) as described in Section 2.3 is a further indication of diverging field lines. No quantitative evaluation of the height gradient has however yet been made.

Other indirect evidence for rapid spreading of the field lines with height is obtained from the observation that the brightness structures become coarser higher up in the atmosphere (Hale and Ellerman, 1903; Simon and Noyes, 1971; Dunn and Zirker, 1973). It is not clear, however, whether the diameter of a bright element is strictly proportional to the diameter of the flux tube at all heights. Beckers (1963, 1968) finds that the inclination angle to the vertical for spicules and dark fine mottles has a very wide distribution, with an average inclination of about 20° for both phenomena. It is natural to expect that the field lines should show similar inclinations. Deubner (1975) has recently obtained evidence from magnetograph observations that the field vectors have a nearly isotropic distribution in quiet regions.

Mehltretter (1974) finds that some of his bright 'points' are slightly elongated. The wide and narrow-band filtergrams, representing two height ranges in the solar atmosphere, show a relative displacement of the bright points in the direction of elongation, indicating a tilt against the normal. Strong tilts of facular elements have also been reported by Stoyanova (1970) and Krat (1973).

2.10. Non-network magnetic fields and possible magnetic turbulence

In Section 2.3 we came to the conclusion that practically all the magnetic flux through the Sun seen by a magnetograph aperture of $2.4 \times 2.4''$ or larger is in the form of strong fields associated with line weakenings. This magnetic flux is located in the supergranulation network when it occurs outside active regions. This conclusion does not exclude the possibility that large amounts of flux and strong fields can occur away from the network. The strong non-network field, if it exists, must however be so tangled that opposite-polarity fluxes cancel out so effectively over an area of $2.4 \times 2.4''$ that the net flux recorded by the magnetograph aperture is small compared with the net flux in the network.

Livingston and Harvey (1971) recorded weak fields inside supergranular cells, which had an apparent strength of 0.2–0.3 *mT*. Recently the fields in the cell interiors have been recorded with considerably improved spatial resolution (Livingston and Harvey, 1975). The polarities were found to be mixed and independent of the surrounding, dominating network-field polarity. Many elements appeared bipolar,

although the flux of the two polarities seldom balanced. The apparent fluxes involved were generally quite small.

Such a tangled field is similar to a 'turbulent' magnetic field. If there exists a strong 'turbulent' field on a small scale, which does not contribute significantly to the net flux recorded with the smallest apertures that can presently be used, it will nevertheless reveal itself by its line-broadening effect. The contribution to the line width from magnetic 'turbulence' is proportional to the Landé factor of the spectral line. Unno (1959) tried to measure B_{turb} by comparing the widths of lines with different Landé factors and obtained an upper limit for B_{turb} of about 30 mT. Howard and Bhatnagar (1970) studied if the difference in line width between granular and intergranular regions varied with Landé factor, and concluded that the difference in B_{turb} between granules and intergranular lanes is less than 3.5 mT. Other authors (Steshenko, 1960; Semel, 1962; Leighton, 1965; Livingston, 1968; Beckers and Schröter, 1968b) have tried to find a magnetic field associated with the granulation in the interior of supergranular cells and have been able to place an upper limit of a few mT for such a field as observed with a resolution of the order of one arcsec.

3. Implications of the Small-Scale Magnetic Structure

3.1. Origin of the observed strong fields

There are essentially three different types of forces that may be invoked to explain how locally strong solar magnetic fields can be confined.

(1) Gas pressure.
(2) Dynamic forces.
(3) Electromagnetic forces.

Figure 4, taken from Stenflo (1975), illustrates the difficulties encountered by gas pressure and dynamic pressure in confining the field. The average height of formation of the Fe I λλ 525.0 and 524.7 nm line wings, which are used to determine the strength of the field, is about 100 km above the level where $\tau_0 = 1$ (Lites, 1972). At this level the ambient gas pressure equals the magnetic pressure of a field of about 120 mT (1.2 kG). This is the maximum field strength that can be confined by gas pressure if the flux tube is completely evacuated at this level (zero internal gas pressure). The field strengths deduced from observations exceed this value. Still Spruit (1975) and Parker (1976) manage to confine 200 mT fields by means of gas pressure effects. This is done by assuming active cooling inside the flux concentrations (Parker, 1976), similar to the cooling mechanism in sunspots (Parker, 1974d, e). The cooling makes the flux region more transparent, producing a Wilson depression of about 200 km (Spruit, 1976). The wings of the spectral lines are accordingly formed deeper down in the magnetic regions, where the external gas pressure is large enough to confine the strong fields.

An argument against this idea is that it is difficult to maintain a large temperature difference between interior and exterior when the flux tube is narrow and close to being optically thin ($d \lesssim 200$ km as shown in Section 2.5). The reason is the short radiative relaxation time for an optically thin plasma, 29 s at the 0 km level, and 12 s

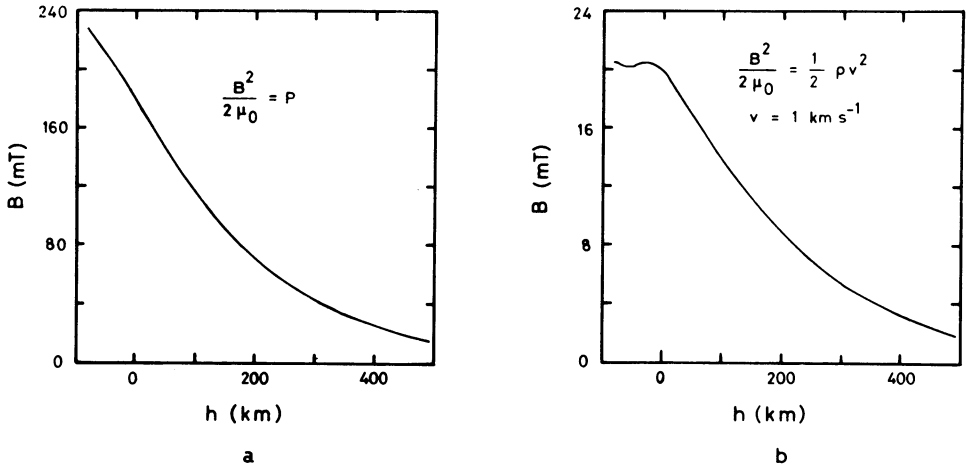

Fig. 4. Variation with height of the field strength that has a magnetic pressure equal to (a) the gas pressure, (b) the dynamic pressure from a flow of 1 km s^{-1}. Pressures and densities are from the facular model of Stenflo (1975).

at the −100 km level (Ulmschneider, 1971). The Wilson depression is expected to increase with optical thickness of the flux tube. The observations of Frazier (1971) show (see Figure 3) that the small isolated flux tubes are physically different from small sunspots in the deeper layers. The temperature deficit in the lower layers in a sunspot is revealed by a corresponding brightness reduction in the continuum. In contrast, the isolated flux elements in plages and in the network are *brighter* in the continuum at disk center (cf. Figure 3 and Section 2.8).

In spite of these difficulties, Parker (1976) believes active cooling to be a more likely cause of the field enhancement than any other mechanism he has considered, i.e. longitudinal and transverse aerodynamic drag (Parker, 1974a, 1976), the Bernoulli effect (Parker, 1974b), turbulence at great depth, viscous stresses in a downdraft, and force-free field configurations.

As shown by Figure 4b, the supergranular flow with velocities of 0.3–0.5 km s^{-1} has a kinetic energy density equal to the magnetic energy density of a magnetic field of less than 10 *mT*. Even in the ordinary granulation, where velocities of a few km s^{-1} occur, the kinetic energy density is much less than the observed magnetic energy density. Peckover and Weiss (1972) have however shown that convection may be able to amplify the field to peak magnetic energy densities considerably exceeding the kinetic energy density in the convective flow. Accordingly it is not ruled out that the granular flow may contribute significantly to maintaining the field confined.

There remains the possibility that the magnetic flux may be confined by internal rather than external forces, by the constricting, pinching forces of longitudinal electric currents (corresponding to a twisted flux-rope), as advocated by Stenflo (1974b, 1975) and Piddington (1975a, c). Indications that twisted fields are a common phenomenon on the Sun come from a variety of observations. The Hα fibrils around sunspots often show a vortex pattern (Hale, 1908, 1927; Richardson, 1941). Observations of transverse magnetic fields (e.g. Severny, 1965; Kotov, 1970)

show strong vertical electric currents in active regions. The time sequence of orientation angles for evolving arch filament systems (Frazier, 1972; Weart, 1972) indicate strong twists. Vorphal (1974) measured 2–3 twists in a length of (2-3)$\times 10^4$ km of an emerging filament. All these observations relate however to relatively large-scale structures. There is presently no direct observational evidence relevant to the question whether all the subarcsec flux tubes are twisted or not.

Parker has rejected force-free fields in his discussion of field confinement, because he believes that twisting cannot enhance the field (Parker, 1976). On the other hand Sreenivasan (1973a, b) and Sreenivasan and Thompson (1974) have shown that certain types of flows, so-called hydromagnetic Beltrami flows, preserve the force-free character of the magnetic field in a resistive medium, and can amplify the fields far beyond equipartition between magnetic and kinetic energy. Part of the reason for this apparent discrepancy between Parker and Sreenivasan appears to be that Parker considers force-free fields in hydrostatic equilibrium through the equation

$$(\nabla \times \mathbf{B}) \times \mathbf{B} = \mathbf{0}, \tag{26}$$

while Sreenivasan treats the general case of dynamic force-free fields with velocity fields in a resistive medium, including the evolution of the field through the equation

$$\frac{\partial \mathbf{B}}{\partial t} = \nabla \times (\mathbf{v} \times \mathbf{B}) + \frac{1}{\mu_0 \sigma} \nabla^2 \mathbf{B}. \tag{27}$$

Stenflo (1974b, 1975) has suggested that Sreenivasan's mechanism can contribute to amplification of the small-scale solar magnetic fields through vorticity flow around the downdrafts (hydromagnetic tornado effect). The Beltrami type of flow can be similar to the whirl in a bath-tub when water goes down the drain. The flux concentrations on the Sun are always cospatial with sinks in the flow (see Section 2.7), located in the intergranular lanes at the supergranular cell boundaries. Vorticity around these sinks may be generated by colliding pressure fronts, likely to occur in a dynamic, inhomogeneous atmosphere, by turbulent shear, and to some extent by Coriolis forces.

So far we have only discussed how the magnetic field may be confined in quasi-stationary flux tubes in the photosphere, and how the field may be amplified in or near the surface layers of the Sun. Parker (1976) has argued that all the amplification from about 10 to 200 mT must in fact take place at the surface or immediately below, since flux tubes are buoyant, and strong fields rise to the surface at nearly the Alfvén speed (Parker, 1955; 1974c). Accordingly fields substantially stronger than 10 mT can hardly be retained in the convection zone.

Contrary to this Piddington (1975a, c) believes that all amplification takes place in the convection zone by differential rotation producing toroidal magnetic flux, which is subsequently rolled into helically twisted flux ropes. Piddington suggests that the typical field strength in the flux ropes in the convection zone is 400 mT.

If not all the field amplification takes place in the convection zone, it is clear that most of the preamplification must occur there. Otherwise the flux would first emerge in a diffuse form, contrary to observations (see Section 2.3). Let x be the fraction of

surface magnetic flux, which at any given time occurs in the form of fields stronger than 100 mT, and let τ be the average life-time of such fields. Let us further assume that the magnetic flux first emerges in the form of fields weaker than 100 mT, and that it takes an average time τ_a to amplify them to fields stronger than 100 mT. Assuming that the magnetic flux is eliminated when the strong flux elements die, and that this flux is replaced by new flux emerging from below, we have in a stationary situation

$$x = \frac{\tau}{\tau_a + \tau}, \tag{28}$$

or

$$\tau_a = \frac{1-x}{x}\,\tau. \tag{29}$$

According to Sections 2.3 and 2.6, $1-x$ may be estimated to be of the order of 10% or less, while τ is about 10 min, assuming that the magnetic flux is destroyed when the cospatial bright points disappear. With these values we get an amplification time $\tau_a \approx 1$ min which is extremely short. In this time an Alfvén wave would travel of the order of 200 km only, and granular motions even less. The observation that only a very small fraction of the total magnetic flux is seen in diffuse form in the photosphere strongly supports the idea of Piddington (1975a, c) that in fact *all* the amplification of the field must occur in the convection zone before the field appears in the photosphere, in spite of Parker's arguments about the buoyancy of flux tubes. Some of the effects we have been discussing, like gas and dynamic pressure effects, vorticity, etc., might play some role down in the convection zone as well, although their contribution to field amplification in the photosphere is likely to be marginal.

When the smallest magnetic elements disintegrate at the end of their life-time τ, it really seems that their flux is completely eliminated from the photosphere, because a mere dispersion of the field lines would be observed as a diffuse field. Such a fast flux elimination is however presently not physically understood.

Finally a word of caution again: The conclusion that all the field amplification occurs below the photosphere rests on the order-of-magnitude correctness of our estimates of $1-x$ and τ in (29), and on the assumption that the flux disappears after time τ, which in turn is justified by our estimated small value of $1-x$. The estimate of τ rests mainly on Mehltretter's (1974) study of the life-time of bright facular points, and on the observation that the flux concentrations always appear to be associated with such bright points, as discussed in Section 2.8. If the strong fields were considerably more long-lived than the bright points, a substantial fraction of the strong-field flux as observed at any given time would be unrelated to bright points or line weakenings, which seems to contradict observations. Nevertheless our estimates of x and τ need verification by new observations.

3.2. Heating of the Solar Atmosphere

Magnetic fields play a role in the energy balance of the solar atmosphere in a variety of ways. Some of the most important are:

https://doi.org/10.1017/S0074180900008081 Published online by Cambridge University Press

(1) Dissipation of magnetic energy, related to the elimination of magnetic flux.
(2) Generation and guiding of MHD waves, which heat the higher layers.
(3) Channelling the heat conduction from the corona.
(4) Causing spicules.

For a given magnetic flux Φ through a surface area A, the lowest energy state corresponds to the situation when the flux is evenly spread out over the area. In that case the average magnetic energy per unit volume in the area, $\bar{W}_{M,\min}$, is

$$\bar{W}_{M,\min} = \bar{B}^2/2\mu_0, \tag{30}$$

$\bar{B} = \Phi/A$ being the average field strength. If we instead have an inhomogeneous distribution, with fields of strength B_0 covering a fraction α of the area, while the rest of the area has zero field, we get

$$\bar{W}_M = \alpha B_0^2/2\mu_0. \tag{31}$$

As

$$\bar{B} = \alpha B_0 \tag{32}$$

we can eliminate α from (31), yielding

$$\bar{W}_M = \bar{B}B_0/2\mu_0, \tag{33}$$

or, using (30),

$$\bar{W}_M = \frac{B_0}{\bar{B}} W_{M,\min}. \tag{34}$$

In quiet regions, with a typical value for $\bar{B}$ of 0.4 mT, and with B_0 in the strong-field elements estimated at 120 mT, the average magnetic energy density exceeds the energy density in a uniformly spread out field with the same magnetic flux by a factor of about 300.

A flux rope with a radius of 100 km and a field strength of 100 mT has a magnetic energy stored within 1000 km along the rope of about 10^{20} J if it is untwisted, more if it is twisted. A twisted, long flux rope may easily contain a magnetic energy of 10^{21} J in the solar atmosphere, which equals the total energy released during a small solar flare, although it carries only a very small amount of magnetic flux. If the annihilation or untwisting of such a flux filament were the cause of a solar flare, a solar magnetograph would hardly notice any changes in the longitudinal magnetic flux. Instead, fictitious flux changes may be recorded, related to line weakenings caused by flare heating (cf. Frazier and Stenflo, 1972; Stenflo, 1974b).

The total number of small flux elements on the Sun was estimated at about 300 000 or more in Section 2.4. This would correspond to a magnetic energy in the solar atmosphere of 10^{26}–10^{27} J. If the magnetic energy in each element is eliminated in as short a time as about 10 min indicated by Mehltretter's (1974) observations (see Section 2.6), the rate of energy dissipation averaged over the solar surface is of the order of 10^5 J m^{-2} s^{-1}. This must however be regarded as an upper limit, since far from all the magnetic flux is in the form of the smallest elements corresponding to bright points, and larger elements have longer life-times (see Section 2.6). Still it is interesting to note that this upper limit is about two orders of magnitude more than is

needed to heat the outer layers of the solar atmosphere. The net radiative energy loss from the chromosphere is $(2–6)\times10^3$ J m^{-2} s^{-1}, while the energy loss from the corona due to radiation and solar wind but ignoring heat conduction downwards to the chromosphere is 55–350 J m^{-2} s^{-1} according to Bray and Loughhead (1974), who give further references. The heating of the solar atmosphere might thus be accounted for, at least partially, by the dissipation of magnetic energy. This energy transformation may occur by dissipation of magnetic flux, or by unwinding of helically twisted fields.

The flux concentrations will also provide heating by MHD waves travelling up along the field lines, generated by the interaction between convection and the magnetic field (Piddington, 1973; Stenflo, 1975). The height variation of the temperature excess in magnetic elements (see Section 2.8) resembles what would be expected by MHD wave heating (Osterbrock, 1961; Milkey, 1970). It is not clear, however, how much this heating contributes to the overall heating of the solar corona.

The relation between flux concentrations and spicules has been touched upon in Section 2.8. It was pointed out that only one spicule should be ejected from each flux element, because the life-time of the field concentration does not seem to exceed the spicule life-time. The excess gas pressure due to efficient heating by MHD waves may be released by outward expansion of the over-heated plasma along the field lines. If these field lines are twisted, the ejected plasma will get a spinning motion (Stenflo, 1974b, 1975). The inclined emission lines of spicules have been interpreted in terms of spinning (Michard, 1956; Beckers *et al.*, 1966; Pasachoff *et al.*, 1968), with rotational velocities at the periphery of the spicules of as much as 30 km s^{-1}, comparable in magnitude with the velocity along the spicule axis.

In small bipolar regions with field-lines in the form of closed loops, the over-heated plasma cannot escape and accumulates at the top of the loop. This may explain the X-ray bright points (Golub *et al.*, 1974), which are cospatial with ephemeral active regions (Harvey and Martin, 1973; Harvey *et al.*, 1974).

3.3. Differential rotation

Two important results obtained from observations of solar rotation are:

(1) The magnetic fields rotate faster by about 5%, i.e. 0.1 km s^{-1} at the equator, than the photospheric plasma (Howard and Harvey, 1970; Wilcox and Howard, 1970; Wilcox *et al.*, 1970; Stenflo, 1974a).

(2) The fields outside active regions (background fields) show a latitude variation of angular velocity more similar to rigid rotation than the active-region fields (Wilcox and Howard, 1970; Wilcox *et al.*, 1970; Stenflo, 1974a). The angular velocity of the various fields agree at the equator, where the maximum angular velocity occurs.

The difference in rotation between the magnetic field and the plasma implies that the magnetic flux cannot be smoothly spread out over the solar surface. The high electrical conductivity in the photosphere prevents slippage of the field lines over a large scale at the required rate. As it is now known that most of the magnetic flux seen by solar magnetographs is in the form of strong fields occupying only a small fraction of the solar surface, the discrepancy between the rotational velocities can be

understood without invoking field-line slippage. The observations of Doppler shifts refer to average line profiles determined mainly by non-magnetic regions (non-magnetic in the sense that they do not contribute significantly to the flux recorded by a magnetograph). The plasma within the strong-field regions, which carry most of the magnetic flux, may well be approximately at rest with respect to the field lines, although the surrounding photospheric plasma may stream with a velocity of about 0.1 km s^{-1} in the eastward direction relative to the flux tubes (Foukal, 1972; Stenflo, 1974a).

The flux tubes can be regarded as rigid columns, exerting a viscous drag on the surrounding photospheric plasma. The effect of this drag is smaller, the smaller the cross-section of the tube. If the flux tubes are anchored in deeper, faster-rotating layers, their drag will tend to speed up the photospheric layers. Foukal and Jokipii (1975) estimate that the spin-up time t due to viscous drag of the flux tubes is

$$t \approx d/(\alpha v), \tag{35}$$

where d is the diameter of the flux tube, v is the relative velocity between the tube and the surrounding plasma, and α is the fraction of the solar surface covered by flux tubes. For d we can use 150 km (see Section 2.5). $v \approx 0.1$ km s^{-1}. α can be estimated in the following way: The total magnetic flux through the solar surface is typically 10^{15} Wb as observed with a $17 \times 17''$ magnetograph aperture (Howard, 1974). This corresponds to an average field of 10^{15} Wb$/4\pi R_\odot^2 \approx 0.16$ mT. Assuming that the true average field strength (not the peak) is 100 mT (see Section 2.1.2.) in the flux tubes, and that they carry most of the magnetic flux, $\alpha \approx 0.16\%$. With these values, the spin-up time becomes $t \approx 10^6$ $s \approx 10$ days. Foukal and Jokipii (1975) arrive at the same value for t by using $d = 1000$ km and $\alpha = 1\%$.

In spite of this extremely rapid spin-up, the velocity difference between the magnetic regions and the rest of the photosphere is observed to be maintained. Foukal and Jokipii (1975) explain this in terms of convection, which transports angular momentum. They point out that the spin-up by the flux tubes can be effective only if it is fast compared with the convective period, and note that the life-time of supergranular cells is only about 10^5 s, much shorter than t. An alternative explanation is given by the life-time of the magnetic structures, which seems to be as small as 10 min for the smallest structures (see Section 2.6). During this time no appreciable drag effect can be effective.

Finally a few words about the difference in rotation rates between the 'background' magnetic field and the field in active regions. The rotation of surface magnetic fields should reflect the rotation rate of deeper layers in which the fields are anchored or from which they are expelled. As the surface fields rotate faster than most of the photosphere, we can conclude that the angular velocity increases with depth. The angular velocity of the background or quiet-region magnetic fields is systematically higher than for active-region fields, indicating that the background fields are related to layers *deeper* than those associated with active-region fields (Stenflo, 1974a). This means that the background fields can hardly be due to the dispersion or turbulent diffusion of the magnetic flux in active regions, in contradiction with the solar cycle model of Leighton (1964, 1969). The short life-times of the magnetic elements (see Section 2.6) is another strong argument against the back-

ground fields being formed by turbulent diffusion. Instead they appear to be more directly linked to the subsurface sources, which all the time supply new magnetic flux to the solar surface to replace the flux that has been dissipated. This direct link with subsurface sources may account for the rigid rotation properties of magnetic sector structures (Schatten *et al.*, 1969) including the associated coronal holes (Timothy *et al.*, 1975).

3.4. Theories of the solar cycle

Several ways in which our new picture of small-scale magnetic fields influence solar cycle theories have already been touched upon in the present paper. In this concluding section we will comment on the implications of the small-scale fields for:

(1) Mean field electrodynamics.
(2) Relation between active and quiet region magnetic fields.
(3) Role of supergranulation.
(4) Dissipation of magnetic flux.

Modern dynamo theories of the solar cycle are based on the concept of mean field electrodynamics and turbulent diffusion of the field (e.g. Steenbeck and Krause, 1969; Leighton, 1969; Parker, 1970; Stix, 1974). Observations indicate that more than about 90% of the magnetic flux observed in the photosphere is channelled through strong-field elements which occupy only of the order of 0.2% of the solar surface (see Section 2.3). This makes the concept of a 'mean field' fairly meaningless in the photosphere. The field seems to be concentrated in this form before it emerges in the solar atmosphere (see Section 3.1). Hence it is doubtful that the mean-field approach will be much more valid deeper in the convection zone (cf. Piddington, 1975c).

Leighton (1964) and Bumba and Howard (1965) suggest that all the background magnetic fields originate in active regions and are dispersed over the Sun by turbulent diffusion, mainly due to the flow in supergranular cells. This dispersion of the field is one of the main ingredients in Leighton's (1969) solar cycle theory. There are two main arguments against the background fields being formed in this way:

(a) The life-time of magnetic elements (see Section 2.6) appears to be very short in comparison with the time it takes to move an element an appreciable distance across the solar surface.

(b) The more rigid-rotation properties of the background fields indicate that they are generally not associated with active-region magnetic fields (see Section 3.3).

There is also observational evidence for new magnetic flux emerging in quiet regions directly from below (e.g. Sheeley, 1969).

Supergranulation has long been believed to be responsible for the enhancement of the field at the cell boundaries (Leighton *et al.*, 1962; Parker, 1963; Simon and Leighton, 1964). As shown in Section 3.1, the flux should however be in a concentrated, strong-field form already when it emerges from below into the photosphere. Bumba and Howard (1965) conclude that new magnetic flux emerges at the inferred edges of supergranules. More recent observations (Harvey and Martin, 1973; Zirin and Tanaka, 1973) lead to the opposite conclusion: New magnetic flux emerges at random with respect to the inferred cell boundaries.

Piddington (1972, 1975a, b, c) has criticized current dynamo theories because they do not account for the removal of the large amounts of flux generated each solar cycle. Turbulent diffusion does not annihilate the field, it only moves the field lines around. Field annihilation is only possible through true ohmic diffusion, which requires length scales less than about 200 km to be sufficiently effective during a solar cycle. This type of elimination of surplus flux is not understood in terms of the 'mean-field' theories.

Observations indicate however that the magnetic flux is destroyed soon after it has appeared in the photosphere (see Section 2.6). The life-time of a flux concentration is roughly proportional to the amount of flux it contains. The largest flux concentrations, the sunspots, may live for months, while the smallest, individual bright network points, live of the order of 10 min. A larger flux concentration is dissolved by breaking apart (fraying) into smaller flux elements, with a flux loss rate of about 10^7 Wb s^{-1} independent of the amount of flux in the decaying structure (see Section 2.6). This is the rate at which the magnetic flux is transferred from smaller to larger Fourier wave numbers. The time it takes to reach wave numbers sufficiently large for ohmic dissipation to be effective is much smaller than the length of the solar cycle.

References

Alfvén, H.: 1967, in Hindmarsh, Lowes, Roberts, and Runcorn (eds.), *Magnetism and the Cosmos*, Oliver & Boyd, Edinburgh/London, p. 246.
Beckers, J. M.: 1963, *Astrophys. J.* **138**, 648.
Beckers, J. M.: 1968, *Solar Phys.* **3**, 367.
Beckers, J. M.: 1972, *Ann. Rev. Astron. Astrophys.* **10**, 73.
Beckers, J. M., Noyes, R. W., and Pasachoff, J. M.: 1966, *Astron. J.* **71**, 155.
Beckers, J. M. and Schröter, E. H.: 1968a, *Solar Phys.* **4**, 142.
Beckers, J. M. and Schröter, E. H.: 1968b, *Solar Phys.* **4**, 165.
Bray, R. J. and Loughhead, R. E.: 1961, *Australian J. Phys.* **14**, 14.
Bray, R. J. and Loughhead, R. E.: 1974, *The Solar Chromosphere*, Chapman and Hall, London.
Bumba, V.: 1963, *Bull. Astron. Inst. Czech.* **19**, 91.
Bumba, V.: 1967, *Solar Phys.* **1**, 371.
Bumba, V. and Howard, R.: *Astrophys. J.* **141**, 1502.
Caccin, B., Falciani, R., and Donati-Falchi, A.: 1974, *Solar Phys.* **35**, 31.
Chapman, G. A.: 1970, *Solar Phys.* **14**, 315.
Chapman, G. A.: 1974, *Astrophys. J.* **191**, 255.
Chapman, G. A. and Sheeley, N. R. Jr.: 1968, *Solar Phys.* **5**, 442.
Deubner, F. L.: 1975, in C. Chiuderi, M. Landini, and A. Righini (eds.), 'First European Solar Meeting (Florence, February 25–27, 1975)', *Osservazioni e Memorie Osservatorio di Arcetri* **105**, 39.
Dravins, D.: 1974, in R. G. Athay (ed.), 'Chromospheric Fine Structure', *IAU Symp.* **56**, 257.
Dunn, R. B. and Zirker, J. B.: 1973, *Solar Phys.* **33**, 281.
Foukal, P.: 1972, *Astrophys. J.* **173**, 439.
Foukal, P. and Jokipii, J. R.: 1975, *Astrophys. J.* **199**, L71.
Frazier, E. N.: 1970, *Solar Phys.* **14**, 89.
Frazier, E. N.: 1971, *Solar Phys.* **21**, 42.
Frazier, E. N.: 1972, *Solar Phys.* **26**, 130.
Frazier, E. N.: 1974, *Solar Phys.* **38**, 69.
Frazier, E. N. and Stenflo, J. O.: 1972, *Solar Phys.* **27**, 330.
Giovanelli, R. G. and Ramsay, J. V.: 1971, in R. Howard (ed.), 'Solar Magnetic Fields', *IAU Symp.* **43**, 293.
Gokhale, M. H. and Zwaan, C.: 1972, *Solar Phys.* **26**, 52.
Golub, L., Krieger, A. S., Silk, J. K., Timothy, A. F., and Vaiana, G. S.: 1974, *Astrophys. J.* **189**, L93.
Gopasyuk, S. I., Kotov, V. A., Severny, A. B., and Tsap, T. T.: 1973, *Solar Phys.* **31**, 307.

Hale, G. E.: 1908, *Astrophys. J.* **28**, 100.
Hale, G. E.: 1927, Nature **119**, 708.
Hale, G. E. and Ellerman, F.: 1903, *Publ. Yerkes Obs.* **3**, 1.
Harvey, J. W.: 1971, *Publ. Astron. Soc. Pacific* **83**, 539.
Harvey, J. W.: 1974, *Flare Related Magnetic Field Dynamics*, NCAR, Boulder, Colorado, p. 1.
Harvey, J. W. and Hall, D.: 1975, Abstract of Report at the 146th AAS meeting, San Diego, California, 17–20 August, 1975.
Harvey, J. W. and Livingston, W.: 1969, *Solar Phys.* **10**, 283.
Harvey, J., Livingston, W., and Slaughter, C.: 1972, *Line Formation in a Magnetic Field*, NCAR, Boulder, Colorado, p. 227.
Harvey, K. and Harvey, J.: 1973, *Solar Phys.* **28**, 61.
Harvey, K. L. and Martin, S. F.: 1973, *Solar Phys.* **32**, 389.
Harvey, K. L., Harvey, J. W., and Martin, S. F.: 1975, *Solar Phys.* **40**, 87.
Howard, R.: 1971, *Solar Phys.* **16**, 21.
Howard, R.: 1972, *Solar Phys.* **24**, 123.
Howard, R.: 1974, *Solar Phys.* **38**, 59.
Howard, R. and Bhatnagar, A.: 1969, *Solar Phys.* **10**, 245.
Howard, R. and Harvey, J.: 1970, *Solar Phys.* **12**, 23.
Howard, R. and Stenflo, J. O.: 1972, *Solar Phys.* **22**, 402.
Kopecký, M.: 1971, *Bull. Astron. Inst. Czech.* **22**, 343.
Kotov, V. A.: 1970, *Izv. Krymsk. Astrofiz. Obs.* **41**, 67.
Krat, V. A.: 1973, *Solar Phys.* **32**, 307.
Kuz'minykh, V. D.: 1964, *Astron. Zh.* **41**, 692 (*Soviet Astron.* **8**, 551).
Leighton, R. B.: 1964, *Astrophys. J.* **140**, 1547.
Leighton, R. B.: 1965, in R. Lüst (ed), 'Stellar and Solar Magnetic Fields', *IAU Symp.* **22**, 158.
Leighton, R. B.: 1969 *Astrophys. J.* **156**, 1.
Leighton, R. B., Noyes, R. W., and Simon, G.: 1962, *Astrophys. J.* **135**, 474.
Lites, B. W.: 1972, *NCAR Cooperative Thesis No. 28*, University of Colorado and High Altitude Observatory, NCAR, Boulder, Colorado.
Livingston, W.: 1968, *Astrophys. J.* **153**, 929.
Livingston, W. and Harvey, J.: 1969, *Solar Phys.* **10**, 294.
Livingston, W. and Harvey, J.: 1971, in R. Howard (ed.), 'Solar Magnetic Fields', *IAU Symp.* **43**, 51.
Livingston, W. and Harvey, J.: 1975, *Bull. Amer. Astron. Soc.* **7**, 346 (Abstract).
Lynch, D. K., Beckers, J. M., and Dunn, R. B.: 1973, *Solar Phys.* **30**, 63.
Mehltretter, J. P.: 1974, *Solar Phys.* **38**, 43.
Michard, R.: 1956, *Ann. Astrophys.* **19**, 1.
Michard, R.: 1974, in R. G. Athay (ed.), 'Chromospheric Fine Structure', *IAU Symp.* **56**, 3.
Milkey, R. W.: 1970, *Solar Phys.* **14**, 62.
Mullan, D. J.: 1974, preprint.
Osterbrock, D. E.: 1961, *Astrophys. J.* **134**, 347.
Parker, E. N.: 1955, *Astrophys. J.* **121**, 491.
Parker, E. N.: 1963, *Astrophys. J.* **138**, 552.
Parker, E. N.: 1970, *Ann. Rev. Astron. Astrophys.* **8**, 1.
Parker, E. N.: 1974a, *Astrophys. J.* **189**, 563.
Parker, E. N.: 1974b, *Astrophys. J.* **190**, 429.
Parker, E. N.: 1974c, *Astrophys. Space Sci.* **22**, 279.
Parker, E. N.: 1974d, *Solar Phys.* **36**, 249.
Parker, E. N.: 1974e, *Solar Phys.* **37**, 127.
Parker, E. N.: 1976, *Astrophys. J.* (in press).
Pasachoff, J. M., Noyes, R. W., and Beckers, J. M.: 1968, *Solar Phys.* **5**, 131.
Peckover, R. S. and Weiss, N. O.: 1972, *Computer Phys. Communications* **4**, 339.
Piddington, J. H.: 1972, *Solar Phys.* **22**, 3.
Piddington, J. H.: 1973, *Solar Phys.* **33**, 363.
Piddington, J. H.: 1975a, *Astrophys. Space Sci.* **34**, 347.
Piddington, J. H.: 1975b, *Astrophys. Space Sci.* **35**, 269.
Piddington, J. H.: 1975c, *Astrophys. Space Sci.* **38**, 157.
Richardson, R. S.: 1941, *Astrophys. J.* **93**, 24.
Schatten, K. H., Wilcox, J. M., and Ness, N. F.: 1969, *Solar Phys.* **6**, 442.
Schmahl, G.: 1967, *Z. Astrophys.* **66**, 81.
Semel, M.: 1962, *Compt. Rend. Acad. Sci. Paris* **254**, 3978.
Servajean, R.: 1961, *Ann. Astrophys.* **24**, 1.

Severny, A. B.: 1965, *Astron. Zh.* **42**, 217.
Severny, A. B.: 1967, *Izv. Krymsk. Astrofiz. Obs.* **38**, 3.
Severny, A. B.: 1972, in C. de Jager (ed.), *Astrophysics and Space Science Library*, Vol. 29, 38.
Sheeley, N. R. Jr.: 1966, *Astrophys. J.* **144**, 723.
Sheeley, N. R. Jr.: 1967, *Solar Phys.* **1**, 171.
Sheeley, N. R. Jr.: 1969, *Solar Phys.* **9**, 347.
Sheeley, N. R. Jr.: 1971, in R. Howard (ed.), 'Solar Magnetic Fields', *IAU Symp.* **43**, 310.
Shine, R. A. and Linsky, J. J.: 1974, *Solar Phys.* **37**, 145.
Simon, G. W. and Leighton, R. B.: 1964, *Astrophys. J.* **140**, 1120.
Simon, G. W. and Noyes, R. W.: 1971, in R. Howard (ed.), 'Solar Magnetic Fields', *IAU Symp.* **43**, 663.
Simon, G. W. and Zirker, J. B.: 1974, *Solar Phys.* **35**, 331.
Skumanich, A., Smythe, C., and Frazier, E. N.: 1975, *Astrophys. J.* **200**, 747.
Spruit, H. C.: 1976, to be published.
Sreenivasan, S. R.: 1973a, *Physica* **67**, 323.
Sreenivasan, S. R.: 1973b, *Physica* **67**, 330.
Sreenivasan, S. R. and Thompson, D. L.: 1974, *Physica* **78**, 321.
Steenbeck, M. and Krause, F.: 1969, *Astron. Nachr.* **291**, 49.
Stellmacher, G. and Wiehr, E.: 1971, *Solar Phys.* **18**, 220.
Stellmacher, G. and Wiehr, E.: 1973, *Astron. Astrophys.* **29**, 13.
Stenflo, J. O.: 1966, *Arkiv. Astron.* **4**, 173.
Stenflo, J. O.: 1968a, *Acta Univ. Lund.* II No. 1 (= *Medd. Lunds Astron. Obs.* Ser. II No. 152).
Stenflo, J. O.: 1968b, *Acta Univ. Lund.* II No. 2 (= *Medd. Lunds Astron. Obs.* Ser. II No. 153).
Stenflo, J. O.: 1971, in R. Howard (ed.), 'Solar Magnetic Fields', *IAU Symp.* **43**, 101.
Stenflo, J. O.: 1973, *Solar Phys.* **32**, 41.
Stenflo, J. O.: 1974a, *Solar Phys.* **36**, 495.
Stenflo, J. O.: 1974b, *Flare Related Magnetic Field Dynamics*, NCAR, Boulder, Colorado, p. 153.
Stenflo, J. O.: 1975, *Solar Phys.* **42**, 79.
Steshenko, N. V.: 1960, *Izv. Krymsk. Astrofiz. Obs.* **22**, 49.
Steshenko, N. V.: 1967, *Izv. Krymsk. Astrofiz. Obs.* **37**, 21.
Stix, M.: 1974, *Astron. Astrophys.* **37**, 121.
Stoyanova, M. N.: 1970, *Solar Phys.* **15**, 349.
Tanenbaum, A. S., Wilcox, J. M., Frazier, E. N., and Howard, R.: 1969, *Solar Phys.* **9**, 328.
Timothy, A. F., Krieger, A. S., and Vaiana, G. S.: 1975, *Solar Phys.* **42**, 135.
Ulmschneider, P.: 1971, *Astron. Astrophys.* **14**, 275.
Unno, W.: 1959, *Astrophys. J.* **129**, 375.
Vorpahl, J.: 1974, in R. G. Athay (ed.), 'Chromospheric Fine Structure', *IAU Symp.* **56**, 197.
Vrabec, D.: 1971, in R. Howard (ed.), 'Solar Magnetic Fields', *IAU Symp.* **43**, 329.
Vrabec, D.: 1974, in R. G. Athay (ed.), 'Chromospheric Fine Structure', *IAU Symp.* **56**, 201.
Weart, S.: 1972, *Astrophys. J.* **177**, 271.
Wiehr, E. and Wittmann, A.: 1975, private communication.
Wilcox, J. M. and Howard, R.: 1970, *Solar Phys.* **13**, 251.
Wilcox, J. M., Schatten, K. H., Tanenbaum, A. S., and Howard, R.: 1970, *Solar Phys.* **14**, 255.
Wilson, P. R.: 1969, *Solar Phys.* **6**, 364.
Zirin, H. and Tanaka, K.: 1973, *Solar Phys.* **32**, 173.

DISCUSSION

Schröter: I have a comment regarding your 'line-ratio' method and a question regarding your new facular model.

(a) It would be much more convincing if you applied this method to three or more lines of the same multiplet and compared the measured circular polarizations in all lines with 'saturation curves' computed accordingly by solving the Stokes-parameter equations numerically. Why did you not do this? We (Dr Wiehr) at Göttingen intend to follow this line.

(b) You observe apparent fields of ≤ 10 G and arrive after reduction at 2 kG (factor of 200!!). Why did you not perform your measurements by positioning your magnetograph-entrance pinhole on bright Ca^+ fine mottles where the directly observed magnetic field strengths are already 50–200 G? You would have avoided such large corrections!

Stenflo: It is irrelevant to speak of large correction factors, because no such factors are derived or used. The value of about 2 kG for the field strength is determined only from the *slope* of the straight line in the

scatter-plot diagram, regardless of the values of the apparent field strengths. My observations were made in a quiet region at disk center in different parts of the wings of the 5250 and 5247 Å lines. Frazier and I are presently working on data for the same lines, obtained in active regions, where the signal-to-noise is better. These new data indicate the same high values of the field strength. We intend to use other combinations of spectral lines in the future.

Zwaan: Spruit has continued his calculations on models of flux tubes. One of these results is that indeed a model explaining intensity and magnetograph data can be found if a flux tube with temperatures lower than the surroundings is embedded in the convection zone and photosphere. Lateral influx affects the structure down to depths over $\tau = 1$ but no longer at substantially larger depths. Of course, as Dr Parker has pointed out, the assumed lower temperature deep down is a dilemma.

Deubner: The figure given by yourself at the blackboard for the flux dissipation rate raises a serious problem as I pointed out already at the Florence meeting: If you take this number at face value, i.e. if the flux was really dissipated or destroyed, it had to be replaced either from below or by random walk processes from sunspot regions at a rate of 10^3 times higher than the average rate of production of active regions. We are led to assume, therefore, that rather than being destroyed the magnetic flux elements are squeezed and juggled around by granular motions. This conclusion is in fact corroborated by observations of white light faculae at high angular resolution, as e.g. published by Mehltretter.

Stenflo: The life-time of the bright points observed by Mehltretter was 5–15 min. If the associated flux tubes were substantially more long-lived, we find that a large fraction of the magnetic flux at any given time is unrelated to brightness enhancements, which seems to contradict observations. Such flux would correspond to a straight line of different slope in the scatter-plot diagram of magnetic fields observed in two different lines.

Parker: I would like to ask what you had in mind with your statement that the 2000 G flux tubes can be confined by currents, twisting and dynamical amplification, etc. The fact is that no matter what the origin of these flux tubes, the concentration to 2000 G is a mechanical one, involving compression, to a pressure $B^2/8\pi$. I did not understand how you hope to accomplish the compression. Only a force can compress a field. What force do you propose?

Stenflo: My general conclusion was that the production of the strong fields must occur in the convection zone, before they emerge in the photosphere. No significant further amplification should occur at the surface. When discussing confinement mechanisms, I pointed out that electromagnetic confinement (force-free fields) is not ruled out, as Sreenivasan has shown by studying the evolution of force-free fields in a resistive medium.

Giovanelli: There seems to be no problem with confinement of the magnetic field in small magnetic elements. A much smaller pressure is needed in the magnetic tube for pressure equilibrium, and this reduces the opacity greatly, so that we see deeper in the magnetic element than in the magnetic-free photosphere. The external pressure at this depth may be substantially greater than at the normal $\tau = 1$ level. Whether the element appears bright or dark depends on the magnetic flux and the internal pressure (and hence the diameter and opacity); theoretically the smaller fluxes are associated with brighter structures, the larger ones with darker structures in qualitative agreement with Frazier's observations.

Krause: You deny that on the Sun there is a mean magnetic field which is generated by a dynamo mechanism. However, I don't see any possibility to gain magnetic energy in the convection zone of the Sun apart from that by a dynamo mechanism feeding energy in the large scale magnetic field, from where it is transported by the interaction with the convective motion into the small scales. Do you see another mechanism which provides for the magnetic fields in the Sun?

Stenflo: I do not reject dynamo theories in general, I conclude that the approach of a 'mean-field electrodynamics' is not a very meaningful approximation. Further, if we can presently only conceive of one way of generating the magnetic fields, this does not necessarily imply that it must be the correct one.